AJNR

Cerebral Veins: Comparative Study of CT Venography with Intraarterial Digital Subtraction Angiography

Stephan G. Wetzel, Eberhard Kirsch, Klaus W. Stock, Michael Kolbe, Achim Kaim and Ernst W. Radue

AJNR Am J Neuroradiol 1999, 20 (2) 249-255
http://www.ajnr.org/content/20/2/249

AJNR Am J Neuroradiol 20:249–255, February 1999

Cerebral Veins: Comparative Study of CT Venography with Intraarterial Digital Subtraction Angiography

Stephan G. Wetzel, Eberhard Kirsch, Klaus W. Stock, Michael Kolbe, Achim Kaim, and Ernst W. Radue

BACKGROUND AND PURPOSE: **Our objective was to compare the reliability of CT venography with intraarterial digital subtraction angiography (DSA) in imaging cerebral venous anatomy and pathology.**

METHODS: **In 25 consecutive patients, 426 venous structures were determined as present, partially present, or absent by three observers evaluating CT multiplanar reformatted (MPR) and maximum intensity projection (MIP) images. These results were compared with the results from intraarterial DSA and, in a second step, with the results of an intraobserver consensus. In addition, pathologic conditions were described.**

RESULTS: **Using DSA as the standard of reference, MPR images had an overall sensitivity of 95% (specificity, 19%) and MIP images a sensitivity of 80% (specificity, 44%) in depicting the cerebral venous anatomy. On the basis of an intraobserver consensus including DSA, MPR, and MIP images (415 vessels present), the sensitivity/specificity was 95%/91% for MPR, 90%/100% for DSA, and 79%/91% for MIP images. MPR images were superior to DSA images in showing the cavernous sinus, the inferior sagittal sinus, and the basal vein of Rosenthal. Venous occlusive diseases were correctly recognized on both MPR and MIP images. Only DSA images provided reliable information of invasion of a sinus by an adjacent meningioma.**

CONCLUSION: **CT venography proved to be a reliable method to depict the cerebral venous structures. MPR images were superior to MIP images.**

The development of helical CT technology offered a new imaging technique to depict the cerebral vascular circulation. The first applications of CT angiography were for the evaluation of the circle of Willis and the detection of aneurysms (1, 2). Recently, the venous circulation was also evaluated (3–5). The term CT venography was used by Casey et al, who described the technique as a rapid method to depict the intracranial venous circulation with consistently high quality (3). However, the sensitivity and specificity of CT venography to depict venous structures in comparison with digital subtraction angiography (DSA), the established standard of reference, is not known.

The main indication for assessment of venous structures is the clinical setting of suspected venous thromboocclusive disease. MR angiography is currently considered to be the noninvasive test of choice for evaluation of the dural sinus (6). However, flow-related and susceptibility artifacts near the sphenoidal sinus can impair the evaluation of the venous structures. The more invasive arterial DSA is still the standard of reference (7).

The purpose of this study was primarily to evaluate the reliability of CT venography in depicting the presence of intracerebral venous structures. We separately compared the findings of DSA images with CT multiplanar reformatted (MPR) images and with the corresponding maximum intensity projection (MIP) images. Then pathologic conditions as displayed by the different imaging techniques were described. The radiation dose for CT venography was measured and the effective dose calculated.

Methods

The findings from 25 consecutive patients (10 men, 15 women) who underwent both intraarterial DSA and CT venography between May 1996 and February 1997 were evaluated to ascertain the presence of the large dural sinuses and the main intracerebral veins.

The patients were 27 to 74 years old (mean, 54 years). The indications for DSA were suspicion of dural sinus thrombosis (four patients), evaluation of a tumor (11 patients), or of a vascular malformation (five patients). In five patients, arterial cerebrovascular disease was investigated. CT venography was performed as an adjunct to routine CT if an enhanced CT scan was indicated before or after DSA. All investigations were

Received May 4, 1998; accepted after revision October 10.

Presented in part at the annual meeting of the American Society of Neuroradiology, Toronto, Canada, May 1997.

From the Department of Diagnostic Radiology, Division of Neuroradiology, University Hospital of Basel, Kantonsspital, Petersgraben 4, 4031 Basel, Switzerland.

Address reprint requests to Stephan Wetzel, MD.

performed with informed consent. DSA (Polytron 1000 S, Siemens, Erlangen, Germany; matrix 512 × 512, 40-cm image intensifier) was performed with a 4F catheter via a femoral arterial approach. The catheter was placed consecutively into both the right and left common or internal carotid arteries in 19 patients. In six patients, only one side was investigated and compared with the other techniques. Contrast material was diluted with 0.9% saline to a concentration of 150 to 250 mg I/mL, and a volume of 7 to 9 mL was injected manually. DSA was performed at two frames per second and included a profile and half-axial projection of each injected artery; thereby, the venous phase was clearly depicted in all investigations. In 16 patients, a basilar angiographic sequence was available. Both investigations were performed within 2 days in 15 patients and between 3 and 10 days in four patients. In six patients, the interval was more than 10 days (up to 8 months); however, these patients had no pathologic conditions of the sinus.

CT venography was performed on a spiral CT scanner with an Advantage Windows 3D workstation. At first, routine unenhanced CT scans were obtained with 5-mm-thick contiguous axial sections through the posterior fossa, followed by 10-mm-thick contiguous axial sections to the vertex. Scan direction for CT venography was from the vertex to the skull base. Scans were angled parallel to a line drawn from the posterior margin of the foramen magnum to the superior margin of the orbita to exclude the lens. The pitch was chosen variably (2.0 to 2.5) to cover the whole distance at a collimation of 1 mm without a tube-cooling delay. Scanning was performed by using 120 kV, a maximum tube current of 220 mA, and a 23-cm display field of view. A total of 100 mL of nonionic contrast material (Iopromidum, [Iodum 300 mg/mL], Schering AG, Germany) was administered at a rate of 3 mL/s by means of a power injector in an antecubital vein. The prescan delay was 40 seconds, and scan duration was 60 seconds. In our previous experience, the injection parameters as described by Casey et al (3) resulted in an excellent opacification of the cerebral veins. The prospective images were reformatted to images with 1-mm collimation and 1-mm spacing; the data were then transferred to the workstation for 3D reconstruction. For MIP images, the bony structures of the image volume had to be removed. This was done by using the adequate threshold for each scan (in our patients, 180–520 HU) to mark only the bone and not any part of the contrast medium–filled sinus. In a second step, the bone model obtained was subtracted from the primary model. The detailed postprocessing steps, the graded subtraction method, is described by Casey et al in detail (3). MIP images were calculated at 30° increments for 180° for one rotation axis (head to feet). In addition, a superior-to-inferior view was displayed, for a total of seven projection images. The reconstruction steps were applied for the whole model; no additional reconstructions of selective parts of the volume (targeted MIP) were performed. The 120 to 150 reformatted images of all three planes per patient were stored on an optical disk and later interpreted on the workstation.

The presence of the venous segments on DSA images was ascertained by one neuroradiologist, a second evaluated the reformatted images in axial, coronal, and sagittal planes on the monitor of the workstation, and a third, the MIP images. All three neuroradiologists independently evaluated one technique each. They were blinded to the results of the other imaging techniques. The only common knowledge was the patient's name, birth date, and examination date. The venous structures evaluated were the superior sagittal, the inferior sagittal, the straight sinus, and the vein of Galen. On both sides, the transverse, sigmoidal, and cavernous sinuses, and the internal cerebral, septal, thalamostriate, and basal Rosenthal veins were assessed, for a total of 18 venous structures. In six patients, only one side was investigated by DSA. In these patients, the contralateral internal venous structures (the internal cerebral, septal, thalamostriate, and basal Rosenthal veins) were not assessed. In all, 426 venous structures were reviewed, each marked as present, partially present, or not present. Additionally, the pathologic conditions were described. At the end of the study, the results of the three examination forms were compared. Interobserver variability was investigated from 10 randomly chosen patients (168 venous structures); thus, every reader evaluated a second technique.

First, the sensitivity, specificity, and positive and negative predictive value for depiction of the venous structures were calculated separately for MPR images and for the MIP images, using DSA images as the standard of reference. Second, an interobserver consensus was used as the standard of reference. A venous structure was considered to be present if depicted clearly and unequivocally on at least one imaging technique. Specificity, sensitivity, and positive and negative predictive value were calculated for DSA, MPR, and MIP images.

The radiation dose for the CT venography protocol was measured with the use of a phantom. The calculated effective dose was compared with the unenhanced CT examination. The radiation dose from standard angiography was not measured.

Results

Comparison with DSA as the Standard of Reference

In 25 consecutive patients, no motion artifacts were observed on CT scans. With DSA, motion artifacts occurred in four patients. All these investigations had diagnostic value. The venous structures determined to be visible, partially visible, or not visible on each of the imaging techniques are listed in Table 1. Using DSA as the standard of reference and considering partially visible venous structures as present, we calculated sensitivity and specificity for the MPR and MIP images. DSA depicted 372 vessels as present and 54 as absent. The MPR images showed correctly 353 of 372 venous segments (sensitivity, 95%; positive predictive value, 89%). On MIP images, 298 were depicted correctly (sensitivity, 80%; positive predictive value, 91%). On MPR images, there were 10 true-negative findings and 44 false-positive findings (specificity, 19%; negative predictive value, 35%); on MIP images, there were 23 true-positive findings and 29 false-positive findings (specificity, 44%; negative predictive value, 23%). The detailed results are presented in Table 2. Asymmetry of the transverse sinus was described on DSA images in 11 patients. On CT scans no prominence was attributed to the wrong side when compared with DSA images. No aplasia of a transverse sinus was observed in the study population.

Interobserver Variability

Interobserver variability yielded a κ value of .46 for DSA images, .23 for MPR images, and .79 for MIP images. For MPR images, the κ value was .71 if the basal vein of Rosenthal was not included.

Comparison with Interobserver Consensus as the Standard of Reference

Many of the venous structures not depicted by DSA were unequivocally seen on the CT scans.

TABLE 1: Display of dural sinuses and cerebral veins

Sinus or Vein	Intraarterial DSA			CT MPR Images			CT MIP Images		
	Present	Partially Present	Absent	Present	Partially Present	Absent	Present	Partially Present	Absent
Superior sagittal sinus (n = 25)	25	⋯	⋯	25	⋯	⋯	23	2	⋯
Transverse sinus (n = 50)	48	2	⋯	49	1	⋯	49	1	⋯
Sigmoid sinus (n = 50)	48	⋯	2	48	1	1	48	1	1
Cavernous sinus (n = 50)	28	14	8	50	⋯	⋯	25	6	19
Inferior sagittal sinus (n = 25)	15	2	8	21	3	1	16	5	4
Straight sinus (n = 25)	23	1	1	25	⋯	⋯	25	⋯	⋯
Galen vein (n = 25)	25	⋯	⋯	25	⋯	⋯	25	⋯	⋯
Internal cerebral veins (n = 44)	42	1	1	44	⋯	⋯	35	3	6
Thalamostriate veins (n = 44)	38	⋯	6	35	⋯	9	16	4	24
Septal veins (n = 44)	30	1	13	18	8	18	10	4	30
Basal Rosenthal veins (n = 44)	22	7	15	41	3	⋯	26	3	15
Total (n = 426)	344	28	54	381	16	29	298	29	99

TABLE 2: Dural sinuses and cerebral veins: DSA standard of reference

Sinus or Vein	Intraarterial DSA		CT Source Images		CT MIP Images	
	Present	Absent	True Positive (Sensitivity) (%)	True Negative (Specificity) (%)	True Positive (Sensitivity) (%)	True Negative (Specificity) (%)
Superior sagittal sinus	25	⋯	100	⋯	100	⋯
Transverse sinus	50	⋯	100	⋯	100	⋯
Sigmoid sinus	48	2	100	50	100	50
Cavernous sinus	42	8	100	0	62	38
Inferior sagittal sinus	17	8	100	13	83	14
Straight sinus	24	1	100	0	100	0
Galen vein	25	⋯	100	⋯	100	⋯
Internal cerebral veins	43	1	100	0	86	0
Thalamostriate veins	38	6	87	67	50	83
Septal veins	31	13	55	31	32	70
Basal Rosenthal veins	29	15	100	0	63	29
Total (n = 426)	372	54	95	19	80	44

TABLE 3: Display of dural sinuses and cerebral veins: Interobserver consensus standard of reference for sensitivity

Sinus or vein	Intraarterial DSA (%)	CT MPR Images (%)	CT MIP Images (%)
Superior sagittal sinus (n = 25)	100	100	100
Transverse sinus (n = 50)	100	100	100
Sigmoid sinus (n = 50)	98	100	100
Cavernous sinus (n = 50)	84	100	62
Inferior sagittal sinus (n = 25)	71	100	88
Straight sinus (n = 25)	96	100	100
Galen vein (n = 25)	100	100	100
Internal cerebral veins (n = 44)	98	100	86
Thalamostriate veins (n = 44)	95	88	50
Septal veins (n = 44)	78	65	33
Basal Rosenthal veins (n = 44)	67	100	69
Total (n = 426)	90	95	79

Therefore, in a second evaluation, on the basis of an interobserver consensus, a venous structure was considered to be present if seen clearly on at least one of the imaging techniques. By using that standard of reference, 415 of the 426 venous structures were assessed as present. Using this standard of reference, DSA images showed correctly 372 vessels as present (sensitivity, 90%); MPR images, 396 vessels (sensitivity, 95%); and MIP images, 326 vessels (sensitivity, 79%). On both MPR and MIP images, respectively, one venous segment was detected, which was rated as present by the blinded observer but as absent on the basis of interobserver consensus. In addition, these venous segments were not present on one of the other two imaging techniques, yielding a specificity of 91% both for MPR and MIP images. The specificity for DSA images was 100%. The positive/negative predictive value was 99.7%/10% for MIP images, 100%/21% for DSA images, and 99.8%/35% for MPR images.

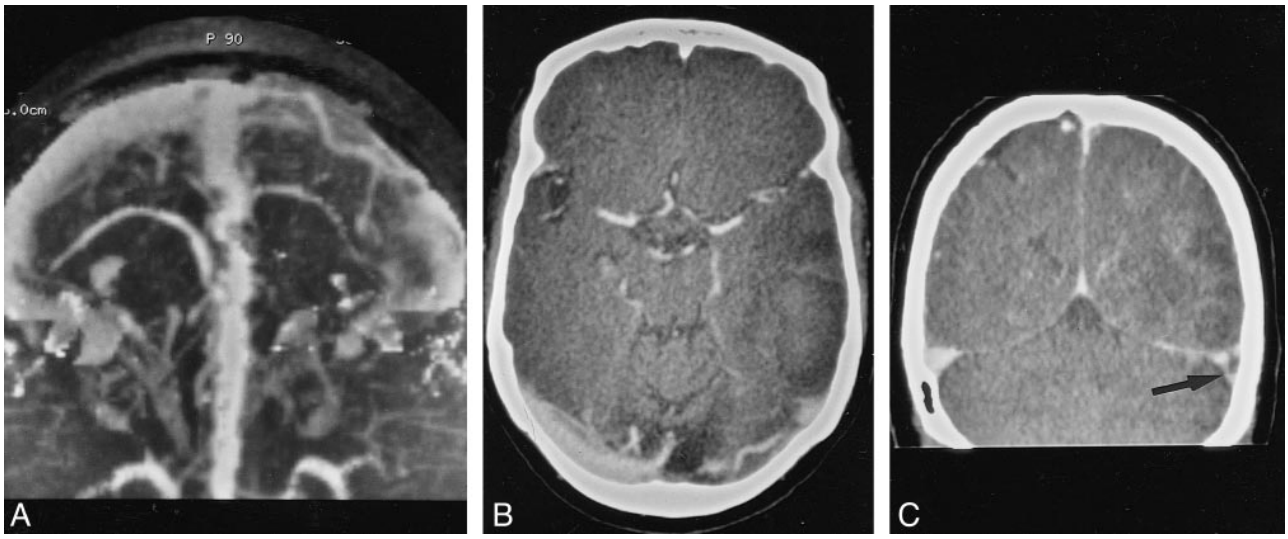

FIG 1. Thrombosis of the left transverse sinus.
A, MIP image (inferior view) shows the irregular filling defect of the left transverse sinus and the collateral venous drainage.
B, MPR image of the same investigation in the axial plane.
C, MPR image in coronal plane provides the same information (*arrow*).

FIG 2. Meningioma adjacent to the superior sagittal sinus.
A, On the DSA image, the invasion of the tumor into the sinus is clearly depicted (*arrow*).
B, Distinction between the enhancing tumor and the contrast medium–filled sinus is not possible on the MPR image.

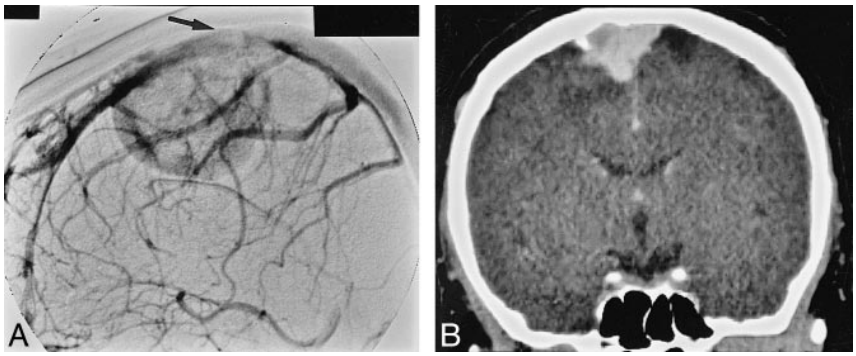

The detailed results for sensitivity are summarized in Table 3.

Occlusive Venous Disease

In one patient, DSA revealed a fresh thrombosis of the left transverse sinus extending into the superior sagittal sinus. Both CT techniques showed the filling defects within the lumen and abnormal collateral venous drainage (Fig 1). A second patient with postthrombotic changes had a greatly narrowed, irregularly configured sinus lumen revealed by both CT techniques and by DSA. In a third patient, an occlusion of the right transverse sinus after embolization of a dural arteriovenous malformation (AVM) was recognized clearly. No false-positive or false-negative findings concerning a dural sinus thrombosis as compared with DSA were described. The sensitivity and specificity in this limited number of cases was 100%. In seven patients, small, sharp, circumscribed, filling defects in a sinus were described on the CT scans, representing arachnoid granulations. Five were located in a transverse sinus, one in the superior sagittal sinus, and one in a sigmoidal sinus. All of them were confirmed by DSA.

Meningiomas

DSA in two patients revealed a tumor with contact to a sinus; both patients had extensive narrowing of the lumen with infiltration. These tumors, as well as the contact to the sinus, were correctly depicted by both CT techniques. It was not possible in either patient to determine whether the tumor invaded the sinus, since both tumors (histologically, meningiomas) showed intense contrast enhancement, making it impossible to accurately define the borders of the sinus at any window level (Fig 2).

Vascular Malformations

Three AVMs and one developmental venous anomaly were detected by DSA. In one patient, DSA revealed a small AVM supplied by the superior cerebellar artery with venous drainage into the straight sinus and cortical veins. Vascular struc-

tures were depicted on MPR and MIP images. Differentiation between an AVM or an anatomic variation was not possible because of metallic artifacts from a surgical clip on an aneurysm at the superior cerebellar artery. A small high-flow AVM detected on DSA images was seen on MPR images as a focus of intense contrast enhancement. A draining vein was only recognized retrospectively. On standard MIP images, that malformation was not detected because of blurring. It was recognized retrospectively on additionally reconstructed targeted MIP images. With this procedure, the small draining vein was depicted, but not the arterial feeders. A partially clipped AVM was not recognized on the CT scans because of metallic artifacts.

A large developmental venous anomaly adjacent to the superior sagittal sinus as depicted on DSA images had, on the CT scans, characteristic findings of radially arranged, dilated anomalous veins converging into an enlarged transcortical ''collector'' vein.

Radiation Dose

The effective dose for the CT venography protocol (pitch, 2.5) was 2.22 mSv and, for the contiguous unenhanced CT scan, 2.48 mSv.

Discussion

For the noninvasive evaluation of the cerebral venous vasculature, a variety of different imaging techniques is available. For unenhanced CT scans in patients with venous sinus thrombosis, the cord sign has been described (8). Although this sign refers to a thrombosed vein, it is rarely encountered. The precontrast CT examination in patients with suspected venous sinus thrombosis serves mainly to depict secondary changes in the brain parenchyma, such as venous infarcts or edema. It also excludes other abnormalities in the initial workup. Contiguous postcontrast CT scans are not reliable for ruling out venous sinus thrombosis. The empty delta sign, an empty triangular shape within the posterior part of the superior sagittal sinus, has been reported to be present only in 29% to 76% of patients with superior sagittal sinus thrombosis or superior sagittal related thrombosis (9, 10). On the other hand, a high splitting sagittal sinus might mimic the appearance of that sign. MR imaging is intrinsically sensitive to flow phenomena and can be applied in all three spatial planes. It has been reported to be very sensitive for diagnosis of a dural sinus thrombosis (11). Yet, because of the number of flow-related artifacts, detailed knowledge of the normal appearance of the sinus as obtained by different sequences is mandatory for correct interpretation. MR angiography is currently regarded as the best noninvasive method for evaluation of the cerebral venous vasculature (6). The major technical drawbacks for the time-of-flight technique are saturation effects occurring at in-plane flow and the inclusion of substances with short T1 relaxation time, such as methemoglobin. In phase-contrast angiography, aliasing artifacts might occur (12). With both techniques, turbulent flow might impair the depiction of a vessel.

The new technique of CT venography provides several advantages. It can be instantly performed as an adjunct to an unenhanced CT scan in patients undergoing the initial workup. A rapid and reliable diagnosis of venous thromboocclusive disease is important, because early therapy is favorable in patients with dural sinus thrombosis (13). Since the scan duration is just 1 minute, the image quality is hardly impaired by patient motion, and patient monitoring is easier in critically ill patients as compared with MR imaging.

In preliminary reports, CT venography has been shown to be a useful method for evaluating the venous structures (3–5). However, the sensitivity and specificity of this method in depicting the venous structures, in comparison with DSA, the established standard of reference, have, to our knowledge, not yet been reported.

In this study, we compared the findings on MPR and MIP images with findings on intraarterial DSA images. This was the standard of reference in the first part of our evaluation. MPR images showed a higher sensitivity (95%) than MIP images (80%) in depicting the venous structures. The specificity was low for both imaging techniques, with 19% for MPR images and 44% for MIP images. The false-positive results were probably attributable to the drawbacks of DSA. If a patent vessel is not seen with DSA, this results in a false-positive finding when the vessel is seen with CT venography. Display of venous structures with DSA could have been improved with more injected contrast medium, more selective catheterization, and additional projections. This was not routinely done. Although the large dural sinuses were depicted with good quality, the frequency of detection of the small cerebral veins was somewhat lower in our study population than is reported in the literature. The thalamostriate vein was seen in 86% of images, the septal vein in 71%, and the basal vein of Rosenthal in 66%. The reported frequency as found in the literature was 92% for the thalamostriate vein, 84% for the septal vein, and 80% for the basal vein of Rosenthal (14, 15). In addition, a ''nonsatisfactory'' depiction of the cavernous sinus was reported in 51% on the conventional carotid angiograms (16). On MPR images, the cavernous sinus was depicted clearly in all patients. Although the angiographic technique was appropriate in the clinical context, it was not optimized for the depiction of venous structures. An optimized angiographic protocol might have changed the results.

To obtain a more accurate standard of reference, on the basis of an interobserver consensus conference, a venous structure was considered to be present if unequivocally seen on at least one imaging technique. Using this standard of reference, MPR

images showed the highest sensitivity (95%), followed by DSA images (90%) and MIP images (79%). On MPR images, the cavernous sinus, the inferior sagittal sinus, and the basal vein of Rosenthal were better depicted. The small septal veins and the thalamostriate veins were better depicted on DSA images.

The lower sensitivity of the MIP display as compared with the source images is probably attributable to the following characteristics: First, an inherent limitation of the MIP algorithm, as described with MR angiography, is that lower-intensity features of the vessels may be lost, leading to an impaired depiction of small vessels (17). It must be assumed that this affects the depiction of the small veins with CT venography as well. Second, although a graded subtraction method was used, a complete subtraction of the thin bone layers at the skull base was not possible without a cutoff of sinus structures because of an overlap in density values. Thus, the evaluation of the cavernous sinus was especially impaired, which was seen on only 62% of MIP images. Third, no targeted MIP reconstructions, which are time-consuming to reconstruct, were used. These probably would have increased the sensitivity and the negative predictive value.

On the basis of this new standard of reference, the sensitivity of CT venography for depiction of the cerebral veins is comparable to DSA. We emphasize that this is true only for the applied angiographic technique and may differ for an angiographic protocol optimized for depiction of the venous structures.

The fresh venous sinus thrombosis as well as the postthrombotic changes and the occlusion of a sigmoidal sinus in three patients were correctly recognized on CT scans. Well-circumscribed filling defects of a large sinus consistent with arachnoid granulations were recognized in seven patients on all imaging techniques. The small size and the otherwise smooth contour of the adjacent sinus helped to differentiate them from thrombosis. The observed frequency and the predominant location in the transverse sinus were in accordance with the findings of a recent investigation in a larger study group, in which arachnoid granulations were found in 24% of contrast-enhanced CT examinations (18).

In two patients with meningiomas, an invasion of the tumor into the sinus was clearly depicted by DSA. CT venography failed in both patients to prove the invasion, since both tumors enhanced as intensely as the sinus, making it impossible to show an infiltration at any window level. Metallic artifacts made the evaluation of two partially clipped AVMs impossible. On contiguous contrast-enhanced CT scans obtained before the present study, the third AVM was seen merely as a focus of intense contrast enhancement. With CT venography, although the characteristics of an intracranial vascular malformation were revealed, the exact architecture, especially the arterial feeders, was not clearly depicted. In these cases, only DSA provided the required information. In comparison, a large developmental venous anomaly was clearly recognized, showing multiple dilated medullary veins converging to a larger transcortical draining vein, giving the ''Medusa head'' appearance, as described recently for CT angiography (19).

CT venography has several advantages over DSA. It is less invasive, less expensive, and the time to diagnosis in the initial workup of a patient is shorter. Pathologic findings of a venous sinus can be displayed either with reformatted images or MIP reconstructions in multiple projections and can be directly related to parenchymal abnormalities. Flow and mixing phenomena of opacified and unopacified blood do not occur, since all venous structures enhance simultaneously. The major limitation of CT venography compared with DSA is the lack of detailed information regarding contrast media flow dynamics. Moreover, metallic artifacts (eg, surgical clips) impair the evaluation of the venous structures to a lesser extent. The reconstruction of MIP images is operator-dependent and time-consuming, and bone structures at the skull base especially impair the evaluation of the cavernous sinus.

Radiation exposure in CT venography is a disadvantage as compared with MR angiography. However, although a small (1-mm) collimation was used, the effective dose was 2.22 mSv, which is lower than that incurred with contiguous unenhanced routine CT (2.48 mSv). The radiation to the lens was additionally reduced by angulating the gantry and thus excluding the orbits from the acquired volume.

Conclusion

CT venography has a high sensitivity for depicting the intracerebral venous circulation. All large sinus were clearly depicted on MPR images as compared with DSA images. All conditions of occlusive venous sinus disease in our limited number of cases were correctly recognized. We are confident that the rapidly feasible CT venographic technique is a good diagnostic tool for the evaluation of suspected dural sinus thrombosis. Time-consuming MIP images provided no added information when compared with the simple MPR images. Recognition of a cerebral vascular malformation is possible, but detailed information about the anatomy of the malformations was only provided by DSA. The depiction of meningioma invasion into a sinus was not reliable, because of the intense enhancement of the tumor itself.

Acknowledgments

We thank J. Roth for the dose measurement, C. Bruederlin and the CT team for their collaboration, and B. Behrmann for secretarial work.

References

1. Alberico RA, Patel M, Casey S, Jacobs B, Maguire W, Decker R. **Evaluation of the circle of Willis with three-dimensional CT angiography in patients with suspected intracranial aneurysms.** *AJNR Am J Neuroradiol* 1995;16:1571–1578
2. Napel S, Marks MP, Rubin GD, et al. **CT angiography with spiral CT and maximum intensity projection.** *Radiology* 1992;185: 607–610
3. Casey SO, Alberico RA, Patel M, et al. **Cerebral CT venography.** *Radiology* 1996;198:163–170
4. Kirchhof K, Jansen O, Sartor K. **CT-Angiographie der Hirnvenen.** *Fortschr Röntgenstr* 1996;165:232–237
5. Hagen T, Bartylla K, Waziri A, Schmitz B, Piepgras U. **Stellenwert der CT- Angiographie in der Diagnostik von zerebralen Sinus- und Venenthrombosen.** *Radiologe* 1996;36:859–866
6. Vogl TJ, Bergman C, Villringer A, Einhaupl K, Lissner J, Felix R. **Dural sinus thrombosis: value of venous MR angiography for diagnosis and follow-up.** *AJR Am J Roentgenol* 1994;162: 1191–1198
7. Chelly D, Levy C, Ameri A, Brunereau L. **Imagerie des thrombophlebites cerebrales.** *Ann Radiol (Paris)* 1994;37:108–117
8. Buonanno FS, Moody DM, Ball MR, Laster DW. **Computed cranial tomographic findings in cerebral sinovenous occlusion.** *J Comput Assist Tomogr* 1978;2:281–290
9. Grosman H, St Louis EL, Gray RR. **The role of CT and DSA in cranial sino-venous occlusion.** *Can Assoc Radiol J* 1987;38:183–189
10. Virapongse C, Cazenave C, Quisling R, Sarwar M, Hunter S. **The empty delta sign: frequency and significance in 76 cases of dural sinus thrombosis.** *Radiology* 1987;162:779–785
11. Dormont D, Anxionnat R, Evrard S, Louaille C, Chiras J, Marsault C. **MRI in cerebral venous thrombosis.** *J Neuroradiol* 1994;21: 81–99
12. Huston J III, Ehman RL. **Comparison of time-of-flight and phase-contrast MR neuroangiographic techniques.** *Radiographics* 1993;13:5–19
13. Einhaupl KM, Villringer A, Meister W, et al. **Heparin treatment in sinus venous thrombosis.** *Lancet* 1991;338:597–600
14. Stein RL, Rosenbaum AE. **Deep supratentorial veins.** In: Newton TH, Potts DG eds. *Radiology of the Skull and Brain, II: Angiography.* St Louis: Mosby; 1974;1903–1998
15. Huber P. *Zerebrale Angiographie für Klinik und Praxis.* 3rd ed. Stuttgart, Germany: Thieme; 1979;208–211
16. Huber P, Huber P. *Zerebrale Angiographie für Klinik und Praxis.* 3rd ed. Stuttgart, Germany: Thieme; 1979;234–235
17. Anderson CM, Saloner D, Tsuruda JS, Shappeero LG, Lee RE. **Artifacts in maximum-intensity-projection display of MR angiograms.** *AJR Am J Roentgenol* 1990;154:623–629
18. Leach JL, Jones BV, Tomsick TA, Stewart CA, Balko MG. **Normal appearance of arachnoid granulations on contrast-enhanced CT and MR of the brain: differentiation from dural sinus disease.** *AJNR Am J Neuroradiol* 1996;17:1523–1532
19. Peebles TR, Pedro PT. **Intracranial developmental venous anomalies: diagnosis using CT angiography.** *J Comput Assist Tomogr* 1997;21:582–586